# Preoperative MRI to predict early recurrence after curative resection of single hepatocellular carcinoma

Chansik An

Department of Medicine

The Graduate School, Yonsei University

# Preoperative MRI to predict early recurrence after curative resection of single hepatocellular carcinoma

Directed by Professor Myeong-Jin Kim

The Doctoral Dissertation
submitted to the Department of Medicine,
the Graduate School of Yonsei University
in partial fulfillment of the requirements for the degree of
Doctor of Philosophy of Medical Science

Chansik An

June 2014

This certifies that the Doctoral Dissertation of Chansik An is approved.

---

Thesis Supervisor : Myeong-Jin Kim

---

Thesis Committee Member#1 : Jin-Sub Choi

---

Thesis Committee Member#2 : Young Nyun Park

---

Thesis Committee Member#3: Chang Hee Lee

---

Thesis Committee Member#4: Do Young Kim

The Graduate School
Yonsei University

June 2014

# ACKNOWLEDGEMENTS

I acknowledge my deep gratitude to Prof. Myeong-Jin Kim, who has been training me in division of gastrointestinal radiology, for supporting my efforts with total commitment and facilitating every step in the process of completing my thesis. My appreciation for his guidance and encouragement is tremendous.

Also, I am indebted to Prof. Jin-Sub Choi, Young Nyun Park, Chang Hee Lee, and Do Young Kim, for their support of me enthusiastically.

Special thanks to Dr. Sung Soo Ahn, for her help providing valuable opinions and discussing enthusiastically to assure the superior quality of this paper.

# <TABLE OF CONTENTS>

# LIST OF FIGURES



# LIST OF TABLES

<ABSTRACT>

Preoperative MRI to predict early recurrence after curative resection of single hepatocellular carcinoma

Chansik An

*Department of Medicine*
*The Graduate School, Yonsei University*

(Directed by Professor Myeong-Jin Kim)

Purpose: Hepatic resection is a primary treatment modality for hepatocellular carcinoma (HCC), but the high incidence of recurrence after hepatic resection remains its major drawback. Especially early recurrence within the first 2 years after resection of HCC is known to be associated with worse prognosis. The purpose of this study was to develop and validate a nomogram based on a multivariate model to preoperatively predict the risk of early recurrence after curative resection of single HCC, using various imaging findings of dynamic gadoxetic acid-enhanced and diffusion-weighted MRI.

Materials and Methods: A total of 268 patients were included who underwent curative hepatic resection for single HCCs followed by gadoxetic acid-enhanced MRI from January 2008 to August 2011. We allocated 187 patients who underwent hepatic resection before September 2010 into the training cohort to derive a prediction model, and the remaining 81 patients were allocated into the validation cohort. All MR images of the training cohort were retrospectively reviewed by two radiologists by consensus, who determined whether the following eight MRI features were found in each HCC: ring-like arterial enhancement, peritumoral arterial enhancement, capsule, peritumoral hypointensity in the hepatobiliary phase (HBP), non-smooth tumor margin in the HBP, satellite nodules, intratumoral fat,

and gross vascular invasion. Based on the multivariate logistic regression analysis, a nomogram was constructed. To validate a prediction model established from the results of the first review, the same radiologists analyzed the MR images of the validation cohort and assessed MRI features that had been independently associated with early recurrence in the training cohort.

Results: Univariate and multivariate logistic regression analyses with 187 patients in the training set showed significant associations between early HCC recurrence and the following factors: ring-like enhancement (odds ratio [OR], 3.83; 95% confidence interval [CI], 1.39-10.52; P=0.01), peritumoral enhancement (OR, 2.64; 95% CI, 1.27-5.46; P<0.009), satellite nodule (OR, 4.07; 95% CI, 1.09-15.21; P=0.037), and tumor size (OR, 1.66; 95% CI, 1.31-2.09; P<0.001). The prediction model based on this result showed an area under the curve (AUC) of 0.791 in the training set. Internal validation with bootstrap sampling was performed to determine calibration accuracy, and the corrected AUC remained high (0.788) after bootstrapping. For the validation data set, discrimination was as good as for the training set, with an AUC of 0.783. The calibration was also good, with no significant difference (P=0.091) between the nomogram-predicted and the observed early recurrence rates.

Conclusion: We developed and validated a nomogram that can be used to preoperatively estimate the risk of recurrence within 2 years after resection of single HCCs.

---

Key words: hepatocellular carcinoma, early recurrence, curative resection, magnetic resonance imaging

Preoperative MRI to Predict Early Recurrence after Curative Resection of Single Hepatocellular Carcinoma

Chansik An

*Department of Medicine*
*The Graduate School, Yonsei University*

(Directed by Professor Myeong-Jin Kim)

## I. INTRODUCTION

Hepatic resection is a primary treatment modality for hepatocellular carcinoma (HCC) in patients with well-preserved liver function.[1,2] However, the high incidence of recurrence after hepatic resection remains its major drawback, with 5-year recurrence rates after curative resection exceeding 50%.[3-5] More than 80% of recurrent tumors develop in the liver remnant, and the mechanisms of this intrahepatic recurrence can be either intrahepatic metastasis from the initial tumor or de novo multicentric occurrence.[6] Of these, intrahepatic metastasis is associated with worse prognosis and usually manifests as early recurrence within the first 2 years after resection of HCC.[7-11] Therefore, the risk factors for early recurrence after hepatic resection have been extensively studied by previous studies. These studies have consistently demonstrated that early recurrence is more likely to be associated with tumor factors such as microvascular invasion, worse histologic differentiation, and microsatellite nodules whereas late recurrence is more likely related to underlying liver conditions such as the presence of cirrhosis.[9,10,12-15] However, most

of these tumor factors can only be evaluated with postoperative pathologic examinations and thus may not be useful in deciding treatment prior to hepatic resection.

The close relationship between early recurrence and tumor factors implies that preoperative imaging findings of HCC could be used to predict early recurrence after hepatic resection. Several studies have evaluated the usefulness of magnetic resonance imaging (MRI) or computed tomography (CT) findings in preoperatively predicting microvascular invasion, a known risk factor for early recurrence, but have yielded conflicting results.[16-21] Other studies demonstrated that early recurrence after resection may be directly related to preoperative imaging findings such as tumor margin and signal intensity (SI) on the hepatobiliary phase (HBP) images of gadoxetic acid-enhanced MRI.[7,18,22]

The purpose of this study was to develop and validate a nomogram based on a multivariate model to preoperatively predict the risk of early recurrence after curative resection of single HCC, using various imaging findings of dynamic gadoxetic acid-enhanced and diffusion-weighted MRI.

## II. MATERIALS AND METHODS

### 1. Patients

The protocol for this retrospective cohort study was approved by our institutional review board and the requirement for written informed consent was waived. From January 2008 to August 2011, 546 consecutive patients underwent curative hepatic resection for HCC at our institution. Of these, 407 patients who met the following criteria were included for this study: (1) gadoxetic acid-enhanced MRI was performed within 2 months before surgery and (2) post-operative pathologic

examination revealed a single HCC. One hundred thirty nine patients were excluded from the study because they had had locoregional therapy such as chemoembolization or chemoradiation prior to surgery (n=105), were followed up for less than 2 years (n=25), died from post-operative complications within two weeks (n=7), or had ruptured HCC (n=2). Therefore, our final study population included 268 patients with 268 HCCs. Before analysis, these patients were divided into two cohorts according to the date of surgery. We allocated 187 patients who underwent hepatic resection from January 2008 to September 2010 into the training cohort to derive a prediction model, and the remaining 81 patients were allocated into the validation cohort. The detailed characteristics of the two cohorts are summarized in Table 1.

**Table 1.** Patient characteristics for the training set and validation sets

| | | **Training Set (n=187)** | **Validation Set (n=81)** | **P-value*** |
|---|---|---|---|---|
| Age (years), mean±SD | | 58.7±10.1 | 57.2±10.4 | 0.27 |
| Male:Female, no. | | 286:72 | 65:16 | 0.936 |
| Child-Pugh class, n (%) | | | | 0.749 |
| | A | 182 (97.3) | 79 (97.5) | |
| | B | 5 (2.7) | 2 (2.5) | |
| Etiology of Liver Disease, no. (%) | | | | 0.571 |

| | | | |
|---|---|---|---|
| HBV | 164 (87.8) | 68 (84) | |
| HCV | 7 (3.7) | 6 (7.4) | |
| Alcoholism | 7 (3.7) | 4 (4.9) | |
| Other | 9 (4.8) | 3 (3.7) | |
| Early recurrence (Yes/No), no. (%) | 56/131 (29.9/70.1) | 30/51 (37/63) | 0.318 |
| AFP (ng/mL), no. (%) | | | 0.749 |
| ≤9 | 65 (41.7) | 27 (38.6) | |
| >9 and ≤400 | 60 (38.5) | 26 (37.1) | |
| >400 | 31 (19.8) | 17 (24.3) | |
| NA | 25 | 11 | |
| PIVKA-II (mAU/ml), no. (%) | | | 0.811 |
| ≤40 | 56 (40.9) | 28 (43.1) | |
| >40 and ≤400 | 48 (35) | 24 (36.9) | |
| >400 | 33 (24.1) | 13 (20) | |
| NA | 44 | 16 | |
| **Qualitative MRI Features (Presence/Absence), no. (%)** | | | |
| Ring-like enhancement | 22/165 (11.8/88.2) | 12/69 | 0.549 |

| | | | |
|---|---|---|---|
| | | (14.8/85.2) | |
| Peritumoral enhancement | 67/120 (35.8/64.2) | 20/61 (24.7/75.3) | 0.006* |
| Capsule | 60/127 (32.1/67.9) | | |
| Peritumoral hypointensity in HBP | 43/144 (23/77) | | |
| Non-smooth tumor margin | 90/97 (48.1/51.9) | | |
| Satellite nodule | 13/174 (7/93) | 9/72 (11.1/88.9) | 0.312 |
| Intratumoral fat | 45/142 (24.1/75.9) | | |
| Gross vascular invasion | 10/177 (5.3/94.7) | | |
| **Quantitative MRI Features, median (range)** | | | |
| Tumor size (cm) | 3.2 (0.8-8.9) | 2.8 (1.1-12.6) | 0.171 |
| SIR on HBP images | 0.4 (0.2-3.3) | | |
| SIR on DWI images | 2.8 (0.9-9.3) | | |
| ADC values ($x10^{-3}$ $mm^2/s$) | 0.9 (0.2-1.5) | | |

For AFP and PIVKA-II, percentages were calculated after excluding non-assessable (missing) cases. * Statistically significant results from Student T-/Mann-Whitney U tests and Fisher's exact/chi-square tests for continuous and categorical variables, respectively. NA: non-assessable, HBP: hepatobiliary phase, SIR: tumor-to-liver

signal intensity ratio, DWI: diffusion-weighted imaging, ADC: apparent diffusion coefficient.

Clinical information, laboratory data, and pathologic reports were retrieved from electronic medical records and were reviewed retrospectively. Clinical information included patient demographics, etiology of chronic liver disease, and time to recurrence. Early recurrence was defined as recurrence within 2 years after curative resection of HCC. Laboratory data included alpha-fetoprotein (AFP) and protein induced by vitamin K absence (PIVKA-II). At our institution, the reference values of AFP and PIVKA-II were <9 ng/mL and <40 mAU/mL, respectively. Pathologic data analyzed in this study were tumor size, the presence of satellite nodules defined as microscopic nodules of HCC separated from the tumor by an interval of non-tumoral liver parenchyma, histologic differentiation, surgical resection margin (invasion or free of tumor), the presence of serosal invasion, and the presence of gross/microscopic vascular invasion.

**2. MRI**

All patients were examined with a 3.0-T MR system (MAGNETOM Trio a Tim; Siemens Medical Solutions, Erlangen, Germany). All images were obtained on the transverse plane using a single dedicated body-phased array coil anteriorly and spinal array coils posteriorly. After the localizer images were obtained, two-dimensional dual-echo T1-weighted spoiled gradient-recalled echo sequence images were obtained during breath-hold (with settings including a repetition time [TR] of 150, effective echo time [TE] of 1.22 for out-of-phase and 2.5 for in-phase, flip angle [FA] of 65 °, one signal acquired, matrix size of 256 x 192, slice thickness of 7 mm and slice gap of 0.7 mm). Pre-contrast and post-contrast dynamic imaging,

including hepatic arterial, portal venous, hepatic venous and final dynamic phase images, were then obtained using a volume interpolated breath-hold examination (VIBE: TR, 2.54 ms; TE, 0.92 ms; FA, 12.3°; matrix size 256 x 192) with a 2-mm interpolated reconstruction. To determine the scan delay of the arterial phase imaging, a bolus technique was utilized with 1-ml gadoxetic acid disodium (Primovist; Bayer Schering Pharma, Berlin, Germany) and a 20-ml 0.9% saline chaser at a 1–2 ml/s injection rate in order to determine the peak enhancement of the abdominal aorta. For dynamic imaging, 0.1 ml/kg (0.025 mmol/kg) of gadoxetic acid disodium was injected, followed by a 20-ml saline chaser at the same rate as that used for the bolus injection. The arterial phase began 2 or 3 s after peak aortic enhancement was determined on the bolus injection; subsequent dynamic images were obtained at approximately 30-s intervals. Each dynamic image acquisition required 18–24 s. Hepatobiliary images were obtained 15–20 min after injection of the contrast agent using the same imaging sequence that was used for the pre- and post-contrast images. Coregistration software (Inline Liver registration, Siemens Medical Solutions, Erlangen, Germany) was used for co-registration of each phase of dynamic contrast-enhanced MRI. During the interval between the dynamic and hepatobiliary phase imaging, T2-weighted images were obtained using a turbo spin echo (TSE: TR/TE 4166.7 ms/88 ms; FA, 150°; matrix size, 256 x 192; slice thickness and gap, 5/1 mm) and diffusion-weighted images (DWI: TR/TE, 1500 ms/70 ms; FA, 90°; matrix size, 192 x 108; slice thickness and gap, 5/1 mm; b-value of 50, 400 and 800) were also obtained. The apparent diffusion coefficient (ADC) for each DWI was automatically calculated by the MR system and displayed as a corresponding ADC map.

**3. Image analysis**

MR images were retrospectively reviewed on a local picture archiving and communication system (PACS; Centricity; GE Healthcare, Milwaukee, WI, USA). One radiologist (C.A.) first recorded the location (liver segment) and corresponding image number of each HCC by reviewing pathologic records, surgical records, and preoperative MR images. With this information two other radiologists (Y.E.C. and H.R. with 11 and 4 years of experience in abdominal MR imaging, respectively), who were unaware of all other clinical, laboratory, and pathologic information, qualitatively and independently determined whether the following eight MRI features were found in each HCC of patients who belong to the training set:

(1) Ring-like arterial enhancement. – defined as the presence of irregular ring-like areas of enhancement with central hypovascular areas in the arterial phase, as described in a previous study (Fig. 1).[23]

(2) Peritumoral arterial enhancement. – defined as a detectable arterial enhancing portion adjacent to the tumor border that later became isointense to the background liver parenchyma in the delayed phase, regardless of its morphologic pattern (e.g. wedge-shaped or circumferential). For this study, we adopted with modifications the definition used in a previous study (Fig. 2).[17]

(3) Capsule. – considered to be present when more than 90% of the tumor circumference was surrounded by a distinct hypointense ring that showed delayed contrast-enhancement.

(4) Peritumoral hypointensity in the HBP. – defined as an irregular, wedge-shaped or flame-like hypointense area of liver parenchyma located outside of the tumor margin in the HBP, as previously described [21].

(5) Non-smooth tumor margin in the HBP. – considered to be present when a tumor had a budding portion at its periphery protruding into the liver parenchyma, as in a

previous study.[18]

(6) Satellite nodules. – defined as nodules that were smaller than 2 cm, located within 2 cm of the main tumor, and showed similar MR characteristics to the main tumor.[24]

(7) Intratumoral fat. – defined as an intratumoral portion that showed signal drop on opposed-phase T1-weighted images compared to in-phase images.

(8) Gross vascular invasion. – considered to be present when a tumor invades adjacent hepatic arteries, hepatic veins, or portal veins.

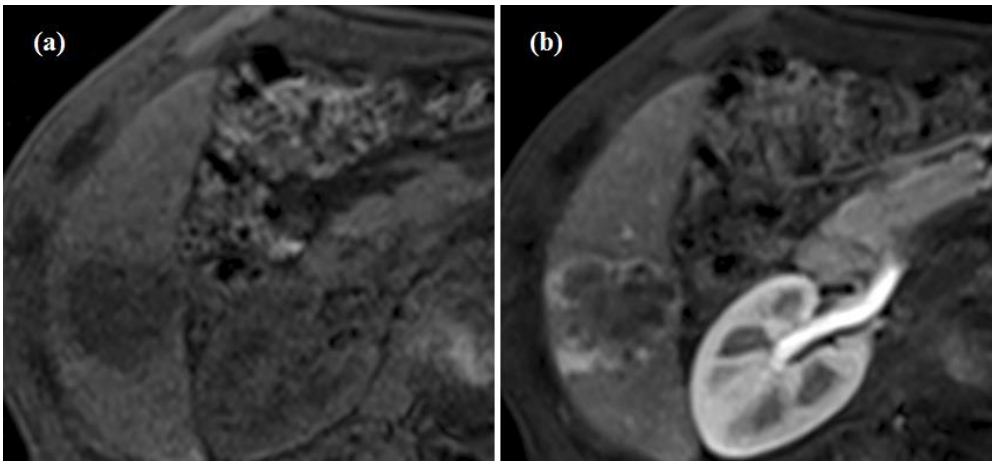


**Figure 1.** Ring-like arterial enhancement. Pathologically confirmed HCC in a 61 year-old man. On unenhanced (a) and arterial phase (b) images of Gd-EOB-DTPA-enhanced T1-weighted MR images, this 4.2 cm tumor shows irregular peripheral arterial enhancement with relatively hypovascular central portions.

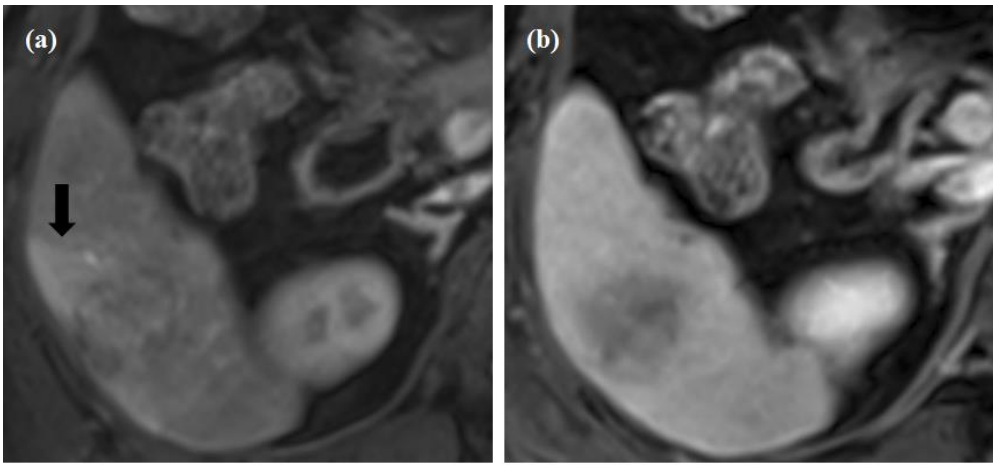


**Figure 2.** Peritumoral arterial enhancement. Pathologically confirmed HCC in a 50 year-old man. In the arterial (a) and venous (b) phases of Gd-EOB-DTPA-enhanced T1-weighted MR images, this 3.5 cm tumor shows the typical enhancement pattern of arterial enhancement and venous washout as well as peritumoral wedge-shaped parenchymal arterial enhancement (arrow) which disappears in the venous phase.

After the first independent image analysis, the two reviewers met together to draw final conclusions by consensus on discordant results. To validate a prediction model established from the results of the first review, the same radiologists analyzed MR images of patients in the validation cohort using the same method described above. For this second review session, however, they only assessed MRI features that had been independently associated with early recurrence in the training cohort.

Quantitative image analysis was performed by a single radiologist (C.A.) who measured the following 4 items for each HCC, in the plane in which the tumor had its largest cross sectional diameter:

(9) Tumor size. – The maximum diameter of each tumor was measured by the

electronic caliper on the PACS.

(10) Signal intensity (SI) ratio on HBP images. – The tumor-to-liver SI ratio was calculated as $SI_{tumor}/SI_{liver}$ on HBP images, where $SI_{tumor}$ is the SI of the tumor and $SI_{liver}$ is the SI of the liver. Regions of interest (ROIs) were placed as large as possible within the confines of the tumor for measuring the mean SI of HCCs. To minimize measurement errors, we used an open source imaging processing package (ImageJ, www.rsb.info.nih.gov) to copy and paste an ROI drawn on HBP images onto the co-registered unenhanced T1-weighted images. The SI of adjacent liver parenchyma was measured using a round ROI (100 $mm^2$ in area) while excluding artifacts and blood vessels.

(11) SI ratio on DWI (b=800). – The tumor-to-liver SI ratio on high b-value DWI was calculated with the same method as described above.

(12) ADC values. – For measurement of ADC value, an ROI was manually drawn on the ADC map to encompass the entire tumor, referencing T2-weighted axial images.

**4. Statistical analysis**

To compare variables between the patients in the training and validation sets, we used Student t- or Mann-Whitney U test for continuous variables and chi-square or Fisher's exact test for categorical variables. Chi-square or Fisher's exact test was used to examine the relationships between pathologic and MRI findings.

Univariate and multivariate logistic regression analyses were used to identify independent determinants of early HCC recurrence. For multivariate regression, multicollinearity between the independent variables was assessed by calculating

variation inflation factors and condition indices. Based on the multivariate logistic regression analysis, a nomogram was constructed. The performance of the nomogram was quantified with respect to discrimination and calibration.[25,26] Discrimination (i.e., whether the relative ranking of individual predictions of subsequent brain metastasis is in the correct order) was quantified with the area under the receiver operating characteristic curve (AUC). We also used the bootstrapping method (200 repetitions) to obtain relatively unbiased estimates. Calibration (i.e., agreement between observed outcome frequencies and predicted probabilities) was first studied with graphic representations (calibration curves), and then it was tested whether the difference between predicted and observed probabilities was significant or not.[26] To compare the discriminative ability between the preoperative prediction model using MRI features and the postoperative prediction model using pathologic findings, pairwise comparison of the AUCs of the two prediction models was performed.

Interobserver agreement on the presence of MRI features was expressed by Cohen's kappa coefficient (k). A kappa statistic of 0.8–1 was considered excellent, 0.6–0.79 good, 0.4–0.59 moderate, 0.2–0.39 fair and 0–0.19 poor agreement [27]. Validity of size measurements obtained using MRI against histologic size measurements was analyzed with the one-way model intraclass correlation coefficient (ICC). The ICC was interpreted as poor (<0.21), fair (0.21-0.4), moderate (0.41-0.6), good (0.61-0.8), or excellent (0.81-1) [28]. Two-sided P-values <0.05 were considered statistically significant. All analyses were performed using SAS version 9.2 (SAS Institute Inc., Cary, NC, USA).

## III. RESULTS

The characteristics of patients in the training set and the validation set are

summarized in Table 1. Between patients in the training and validation sets, no significant difference was found in mean age (about 58 year old), male to female ratio (about 4), Child-Pugh class (most patients [about 97%] were class A), etiology of liver disease (most patients were B-viral carriers; 87.8% for the training and 84% for the validation sets), early recurrence rate (29.9% vs. 37%), and the serum levels of the tumor markers (AFP and PIVKA-II); and the proportions of ring-like enhancement (11.8% vs. 14.8%) and coexisting satellite nodule (7% vs. 11.1%) found on MRI were also similar in both sets. However, peritumoral enhancement was seen more frequently in the validation set (35.8%) than in the trainings set (24.7%) (P=0.0055).

Logistic regression including the variables that are assessable preoperatively (tumor markers and MRI features) was performed to establish a model to predict early HCC recurrence. Univariate analysis with 187 patients in the training set showed that tumor size and the presence of ring-like enhancement, peritumoral enhancement, peritumoral hypointensity on HBP, non-smooth tumor margin, satellite nodule, gross vascular invasion, and >400 mAU/ml (vs. ≤9) of PIVKA-II were significantly associated with early recurrence. The presence of capsule and intratumoral fat on MRI, tumor-to-liver SI ratio on HBP/DWI images, ADC values, and the serum level of AFP were not significantly related to the prognosis (Table 2). When a multiple logistic regression model was fitted to all the variables found to be significant in the univariate analysis, the following risk factors attained statistical significance: ring-like enhancement (odds ratio [OR], 3.83; 95% confidence interval [CI], 1.39-10.52; P=0.01), peritumoral enhancement (OR, 2.64; 95% CI, 1.27-5.46; P<0.009), satellite nodule (OR, 4.07; 95% CI, 1.09-15.21; P=0.037), and tumor size (OR, 1.66; 95% CI, 1.31-2.09; P<0.001). There was no multicollinearity between these independent variables.

**Table 2.** Univariate and multivariate analysis of preoperative MRI findings and tumor markers predicting early recurrence in the training set

| | **Univariate Analysis** | | | **Multivariate Analysis** | | |
|---|---|---|---|---|---|---|
| | OR | 95% CI | P-value | OR | 95% CI | P-value |
| Ring-like enhancement | 3.3 | 1.33-8.18 | 0.009* | 3.83 | 1.39-10.52 | 0.01* |
| Peritumoral enhancement | 3.27 | 1.71-6.28 | <0.001* | 2.64 | 1.27-5.46 | 0.009* |
| Capsule | 0.7 | 0.35-1.4 | 0.3114 | | | |
| Peritumoral hypointensity on HBP images | 2.97 | 1.46-6.04 | 0.003* | 1.11 | 0.43-2.88 | 0.831 |
| Non-smooth tumor margin | 2.07 | 1.09-3.92 | 0.026* | 1.13 | 0.52-2.44 | 0.765 |
| Satellite nodule | 4.2 | 1.31-13.48 | 0.016* | 4.07 | 1.09-15.21 | 0.037* |
| Intratumoral fat | 0.6 | 0.27-1.31 | 0.197 | | | |
| Gross vascular invasion | 10.75 | 2.2-52.43 | 0.003* | 4.22 | 0.74-24.06 | 0.105 |
| Tumor size (cm) | 1.7 | 1.36-2.11 | <0.001* | 1.66 | 1.31-2.09 | <0.001* |

| | | | | | | |
|---|---|---|---|---|---|---|
| SIR on HBP images | 0.41 | 0.1-1.72 | 0.222 | | | |
| SIR on DWI images | 1.02 | 0.82-1.25 | 0.878 | | | |
| ADC values ($x10^{-3}$ $mm^2/s$) | 1.01 | 0.98-1.03 | 0.889 | | | |
| AFP (ng/mL) | | | | | | |
| ≤9 | | reference | | | | |
| >9 and ≤400 | 2.49 | 0.89-5.54 | 0.079 | | | |
| >400 | 1.91 | 0.72-5.01 | 0.192 | | | |
| PIVKA-II (mAU/ml) | | | | | | |
| ≤40 | | reference | | | | |
| >40 and ≤400 | 1.51 | 0.12-42.09 | 0.133 | | | |
| >400 | 3.06 | 1.19-7.79 | 0.02* | 1.08 | 0.35-3.98 | 0.791 |

* Statistically significant results from logistic regression analysis. OR: odds ratio, CI: confidence interval, HBP: hepatobiliary phase, SIR: tumor-to-liver signal intensity ratio, DWI: diffusion-weighted imaging, ADC: apparent diffusion coefficient.

The formula derived from the results of the multivariate logistic regression model is as following:

The probability of recurrence = 1 / (1 + exp (-3.4113 + 1.3421 x Ring-like

Enhancement + 0.9697 x Peritumoral Arterial Enhancement + 1.4032 x Satellite Nodule + 0.5039 x Tumor Size))

A nomogram to predict early HCC recurrence after resection was constructed based on this formula (Fig. 3). This prediction model showed an AUC of 0.791 in the training set (Fig. 4). Internal validation with bootstrap sampling was performed to determine calibration accuracy, and the corrected AUC remained high (0.788) after bootstrapping (Fig. 5A). We next examined the accuracy of the nomogram in an independent data set of 81 patients. For this validation data set, discrimination was as good as for the training set, with an AUC of 0.783 (Fig. 4). The calibration was also good, with no significant difference (P=0.091) between the nomogram-predicted and the observed early recurrence rates (Fig. 5B).

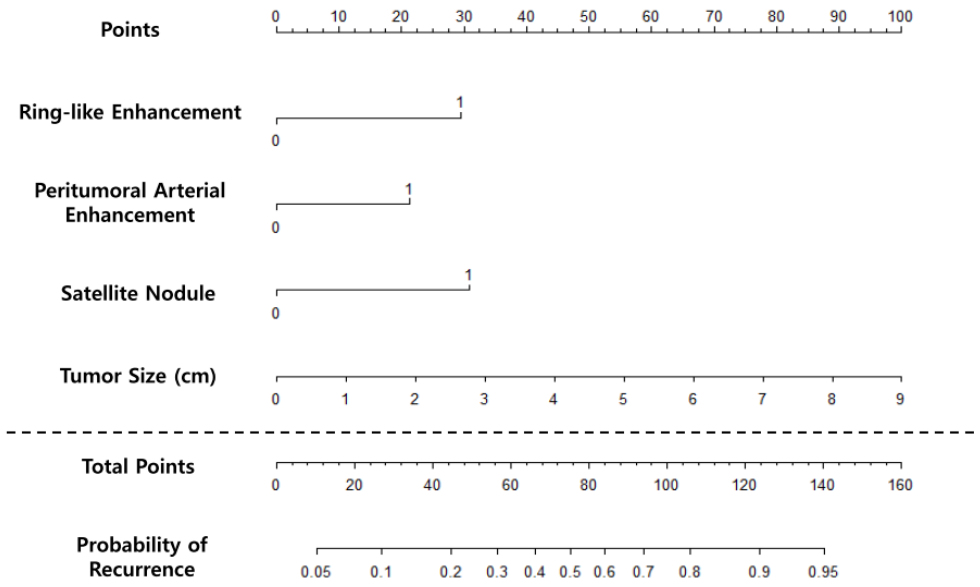

**Figure 3.** Nomogram to predict the probability of recurrence within 2 years after resection of single hepatocellular carcinoma. (Top) Predictor points are found on the uppermost point scale that corresponds with each variable. (Bottom) The points of all variables are added up, and the total point projected on the bottom scale indicates the probability of recurrence.

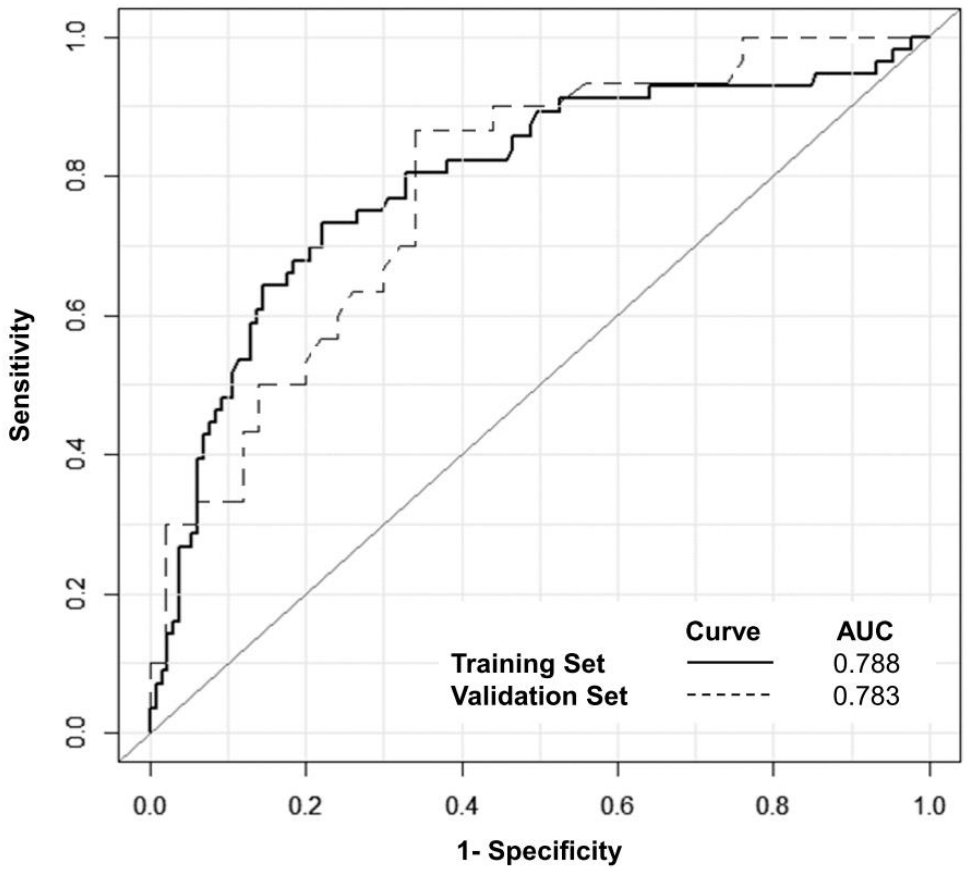


**Figure 4.** The Receiver operating characteristic curves of the prediction model in the training and validation data sets

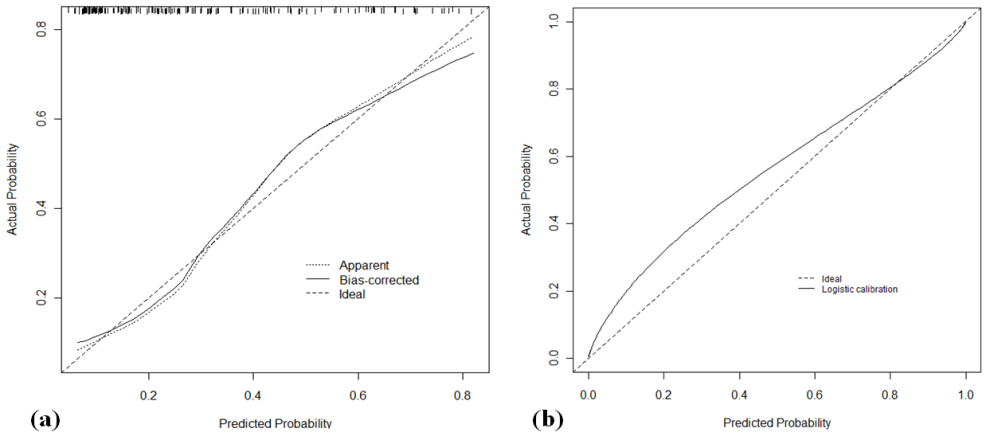


**Figure 5.** Calibration Curves of the preoperative model (nomogram) to predict early recurrence after resection of hepatocellular carcinoma. (a) Predicted and observed recurrence rates are plotted for the training set. The dashed line represents the performance of the ideal nomogram. The dotted and solid lines represent the performance of our nomogram without and with bootstrap correction, respectively. (b) External validation of the nomogram in the training data set.

Univariate and multivariate logistic regression analyses using pathologic findings as variables showed that larger tumor size (OR, 1.45; 95% CI, 1.16-1.81; P=0.001) and the presence of microvascular invasion (OR, 2.87; 95% CI, 1.31-6.33; P=0.009) or satellite nodules (OR, 4.62; 95% CI, 1.12-32.42; P=0.029) were independently associated with the increase risks of early HCC recurrence in the training cohort (Table 3). Histologic differentiation, serosal tumor invasion, and positive resection margin were not significantly related to recurrence. The relationship between gross vascular invasion and early recurrence was statistically significant in the univariate analysis, but not in the multivariate analysis (Table 3). The multivariate prediction model using the pathologic findings (tumor size, microvascular invasion, and

satellite nodule) showed an AUC of 0.763. Pairwise comparison of the AUCs between the MRI and pathologic prediction models showed no significant difference (0.783 vs. 0.763, P=0.621).

**Table 3.** Univariate and multivariate analysis of postoperative pathologic findings predicting early recurrence in the training set

| | **Univariate Analysis** | | | **Multivariate Analysis** | | |
|---|---|---|---|---|---|---|
| | OR | 95% CI | P-value | OR | 95% CI | P-value |
| Histologic differentiation | | | | | | |
| Well | | reference | | | | |
| Moderately | 2.09 | 0.24-18.01 | 0.499 | | | |
| Poorly | 5.06 | 0.61-42.09 | 0.133 | | | |
| Tumor size | 1.56 | 1.28-1.91 | <0.001* | 1.45 | 1.16-1.81 | 0.001* |
| Microvessel invasion | 4.49 | 2.13-9.46 | <0.001* | 2.87 | 1.31-6.33 | 0.009* |
| Gross vascular | 12.65 | 1.44- | 0.022* | 4.13 | 0.38- | 0.247 |

| | | | | | | |
|---|---|---|---|---|---|---|
| invasion | | 110.92 | | | 45.56 | |
| Satellite nodule | 12.56 | 2.55-58.8 | 0.002* | 4.62 | 1.12-32.42 | 0.029* |
| Positive resection margin | 4.78 | 0.42-53.81 | 0.206 | | | |
| Serosal invasion | 2.98 | 0.87-10.19 | 0.083 | | | |

* Statistically significant results from logistic regression analysis. OR: odds ratio, CI: confidence interval, HBP: hepatobiliary phase, SIR: tumor-to-liver signal intensity ratio, DWI: diffusion-weighted imaging, ADC: apparent diffusion coefficient.

Cross tabulation with chi-square or Fisher's exact test revealed that microvascular invasion was significantly associated with ring-like enhancement (OR, 5.46; P=0.005) and peritumoral arterial enhancement (OR, 3.89; P<0.001) (Table 4).

**Table 4.** The relationships between microvascular invasion and two MRI findings (ring-like enhancement and peritumoral arterial enhancement)

| | **Ring-like Enhancement** | | | **Peritumoral Arterial Enhancement** | | |
|---|---|---|---|---|---|---|
| | Presence | Absence | Total | Presence | Absence | Total |

| | | | | | | |
|---|---|---|---|---|---|---|
| Microvascular invasion (+) | 19 | 87 | 106 | 51 | 55 | 106 |
| Microvascular invasion (-) | 3 | 75 | 78 | 15 | 63 | 78 |
| Total | 22 | 162 | 184 | 66 | 118 | 184 |

The number in each cell indicates the number of patients; Of 187 patients, 3 were non-assessable (missing). The odds ratio for microvascular invasion is 5.46 for ring-like enhancement (Fisher's exact test, P=0.005) and 3.89 for peritumoral arterial enhancement (chi-square test, P<0.001).

Interobserver agreements on the presence of the three MRI features that were independently associated with early recurrence were all good: k=0.72 for ring-like arterial enhancement, k=0.738 for peritumoral arterial enhancement, and k=0.721 for satellite nodules. Intermethod agreement between MR readings and pathologic reports on tumor size was excellent; the ICC was 0.93, with a narrow 95% CI (0.91-0.95).

## IV. DISCUSSION

The results of this study demonstrate that a prediction model based on preoperative MRI findings can be a useful tool to estimate the probability of early recurrence after resection of HCCs. Our study cohort was restricted to patients with single HCCs and preserved liver function undergoing curative hepatic resection, through which we aimed at increasing the reliability of our prediction model and clearly specifying its target patient population, because the prognosis of HCC patients

depends not only on tumor factors but also on liver function and treatment modality.

The variables included in our prediction model were tumor size and the presence or absence of ring-like enhancement (Fig. 1), peritumoral arterial enhancement (Fig. 2), and satellite nodule evaluated with MRI. It may help to explain this result if we compare this MRI-based model with another prediction model that we developed using pathologic findings (Tables 2 and 3). These two prediction models were comparable in structure and predictive ability. The pathology-based model has tumor size and the presence or absence of microvascular invasion and satellite nodule as predictors, with a similar AUC to that of the MRI-based model. Among the three predictors of the pathology-based model, microvascular invasion cannot be evaluated with MRI, but the other two variables (tumor size and satellite nodule) were also included in the MRI-based model and showed similar ORs. In the MRI-based model, two MRI findings (ring-like enhancement and peritumoral arterial enhancement) were included in lieu of microvascular invasion. These observations suggest that tumor size and the presence of significant satellite nodule can be accurately with MRI, and that evaluating the two MRI findings could be as helpful for predicting early recurrence as pathologically examining microvascular invasion.

Although this cannot be evidence for direct association between the presence of microvascular invasion and these MRI findings, it is still highly likely that the ability of these MRI findings to predict early HCC recurrence arises partly from their associations with the presence of microvascular invasion. In our study, cross tabulation with chi-square tests showed the significant associations between both of the two MRI findings and the presence of microvascular invasion (Table 4). Previous studies also demonstrated that peritumoral arterial enhancement, or tumorous arterioportal shunt, is a risk factor of microvascular invasion.[16,17,29] There have been a few previous studies on HCCs showing ring-like enhancement, although none has investigated its relationship with microvascular invasion. These

previous studies showed that ring-like enhancement pattern is associated with rapid progression, poor differentiation, and worse prognosis,[23,30,31] which supports our results that this enhancement pattern is significantly associated with the presence of microvascular invasion and the increased risk of early recurrence after resection.

In our study, the presence of gross vascular invasion and the presence of peritumoral hypointense area or non-smooth tumor margin on HBP images were significantly associated with early HCC recurrence in the univariate analysis, but lost their statistical significance with decreased ORs in the multivariate analysis, meaning that their role in predicting early recurrence is non-significant in the presence of other stronger variables (Table 2). Particularly, gross vascular invasion lost its significance in the multivariate analysis even when assessed pathologically, suggesting that the non-significant role of gross vascular invasion is not because of the inaccuracy of MRI evaluation. This result is probably because of the highly-selected patients in this study who were candidates for curative resection, in whom gross vascular invasion may have been less frequent and severe than it would have been in advanced HCCs and thus have no additional impact on the risk of early recurrence.

Tumor-to-liver SI on HBP images, encapsulation, and the presence of intratumoral fat were reported to be directly or indirectly related to prognosis, but showed no significant association with early recurrence in our study population in both the univariate and multivariate analyses. However, our results should not be interpreted as evidence that these MRI features are not associated with prognosis in other HCC patient populations. Indeed, the patient characteristics of most previous studies reporting prognosis of HCCs with these MRI features are different from ours. For instance, as opposed to our study population, patients with compromised liver function were included in some previous studies.[32,33] One previous study showed that HCC encapsulation is a significant prognostic factor only for HCCs >5 cm.[34]

A few previous studies consistently found that higher SI on DWI are associated with worse histologic differentiation, but they reported conflicting results on the relationship between ADC values and histologic differentiation.[35-38] No previous study, to our knowledge, has investigated the direct relationship between tumor SI or ADC on DWI and prognosis. In our study population, neither histologic differentiation nor SI or ADC on DWI was a significant predictor of early HCC recurrence (Tables 2 and 3).

A major limitation to this study is its retrospective nature. We built a model using a training data set and validated it with an independent validation cohort set, in order to increase its reliability. The patients included in this study were still, however, from a single center, and our results may not be generalized across all institutions. Prospective studies with various patient populations will be required to further validate our prediction model.

## V. CONCLUSION

We developed and validated a nomogram that can be used to preoperatively estimate the risk of recurrence within 2 years after resection of single HCCs. Our nomogram may be useful in selecting target patients for resection, establishing the extent of resection, counseling patients, or planning study design for clinical trials.

## REFERENCES


1. Roayaie S, Obeidat K, Sposito C, Mariani L, Bhoori S, Pellegrinelli A, et al. Resection of hepatocellular cancer </=2 cm: results from two Western centers. Hepatology 2013;57:1426-35.
2. Bruix J, Sherman M. Management of hepatocellular carcinoma: an update. Hepatology 2011;53:1020-2.
3. Harada T, Shigemura T, Kodama S, Higuchi T, Ikeda S, Okazaki M. Hepatic resection is not enough for hepatocellular carcinoma. A follow-up study of 92 patients. Journal of clinical gastroenterology 1992;14:245-50.
4. Nagasue N, Uchida M, Makino Y, Takemoto Y, Yamanoi A, Hayashi T, et al. Incidence and factors associated with intrahepatic recurrence following resection of hepatocellular carcinoma. Gastroenterology 1993;105:488-94.
5. Shah SA, Cleary SP, Wei AC, Yang I, Taylor BR, Hemming AW, et al. Recurrence after liver resection for hepatocellular carcinoma: risk factors, treatment, and outcomes. Surgery 2007;141:330-9.
6. Tung-Ping Poon R, Fan ST, Wong J. Risk factors, prevention, and management of postoperative recurrence after resection of hepatocellular carcinoma. Annals of surgery 2000;232:10-24.
7. Lee JI, Lee JW, Kim YS, Choi YA, Jeon YS, Cho SG. Analysis of survival in very early hepatocellular carcinoma after resection. Journal of clinical gastroenterology 2011;45:366-71.
8. Choi G, Kim D, Kang C, Kim K, Choi J, Lee W, et al. Prognostic factors and optimal treatment strategy for intrahepatic nodular recurrence after curative resection of hepatocellular carcinoma. Annals of Surgical Oncology 2008;15:618-29.
9. Portolani N, Coniglio A, Ghidoni S, Giovanelli M, Benetti A, Tiberio GA, et al. Early and late recurrence after liver resection for hepatocellular

carcinoma: prognostic and therapeutic implications. Annals of surgery 2006;243:229-35.

10. Poon RT, Fan ST, Ng IO, Lo CM, Liu CL, Wong J. Different risk factors and prognosis for early and late intrahepatic recurrence after resection of hepatocellular carcinoma. Cancer 2000;89:500-7.
11. Shimada M, Takenaka K, Gion T, Fujiwara Y, Kajiyama K, Maeda T, et al. Prognosis of recurrent hepatocellular carcinoma: a 10-year surgical experience in Japan. Gastroenterology 1996;111:720-6.
12. Imamura H, Matsuyama Y, Tanaka E, Ohkubo T, Hasegawa K, Miyagawa S, et al. Risk factors contributing to early and late phase intrahepatic recurrence of hepatocellular carcinoma after hepatectomy. Journal of hepatology 2003;38:200-7.
13. Kamiyama T, Nakanishi K, Yokoo H, Kamachi H, Tahara M, Kakisaka T, et al. Analysis of the risk factors for early death due to disease recurrence or progression within 1 year after hepatectomy in patients with hepatocellular carcinoma. World journal of surgical oncology 2012;10:107-.
14. Park JH, Koh KC, Choi MS, Lee JH, Yoo BC, Paik SW, et al. Analysis of risk factors associated with early multinodular recurrences after hepatic resection for hepatocellular carcinoma. The American journal of surgery 2006;192:29-33.
15. Cucchetti A, Piscaglia F, Caturelli E, BenvegnApk L, Vivarelli M, Ercolani G, et al. Comparison of recurrence of hepatocellular carcinoma after resection in patients with cirrhosis to its occurrence in a surveilled cirrhotic population. Annals of Surgical Oncology 2009;16:413-22.
16. Miyata R, Tanimoto A, Wakabayashi G, Shimazu M, Nakatsuka S, Mukai M, et al. Accuracy of preoperative prediction of microinvasion of portal vein in hepatocellular carcinoma using superparamagnetic iron oxide-enhanced magnetic resonance imaging and computed tomography during

hepatic angiography. Journal of gastroenterology 2006;41:987-95.

17. Kim H, Park M, Choi JY, Park YN, Kim M, Kim KS, et al. Can microvessel invasion of hepatocellular carcinoma be predicted by pre-operative MRI? European radiology 2009;19:1744-51.

18. Ariizumi S, Kitagawa K, Kotera Y, Takahashi Y, Katagiri S, Kuwatsuru R, et al. A non-smooth tumor margin in the hepatobiliary phase of gadoxetic acid disodium (Gd-EOB-DTPA)-enhanced magnetic resonance imaging predicts microscopic portal vein invasion, intrahepatic metastasis, and early recurrence after hepatectomy in patients with hepatocellular carcinoma. Journal of Hepato-Biliary-Pancreatic Sciences 2011;18:575-85.

19. Chandarana H, Robinson E, Hajdu CH, Drozhinin L, Babb JS, Taouli B. Microvascular invasion in hepatocellular carcinoma: is it predictable with pretransplant MRI? AJR, American journal of roentgenology 2011;196:1083-9.

20. Griffin N, Addley H, Sala E, Shaw AS, Grant LA, Eldaly H, et al. Vascular invasion in hepatocellular carcinoma: is there a correlation with MRI? British journal of radiology 2012;85:736-44.

21. Kim KA, Kim MJ, Jeon HM, Kim KS, Choi J, Ahn SH, et al. Prediction of microvascular invasion of hepatocellular carcinoma: usefulness of peritumoral hypointensity seen on gadoxetate disodium-enhanced hepatobiliary phase images. Journal of magnetic resonance imaging 2012;35:629-34.

22. Choi JW, Lee JM, Kim SJ, Yoon J, Baek JH, Han JK, et al. Hepatocellular Carcinoma: Imaging Patterns on Gadoxetic Acid-enhanced MR Images and Their Value as an Imaging Biomarker. Radiology 2013;267:776-86.

23. Kawamura Y, Ikeda K, Hirakawa M, Yatsuji H, Sezaki H, Hosaka T, et al. New classification of dynamic computed tomography images predictive of malignant characteristics of hepatocellular carcinoma. Hepatol Res

2010;40:1006-14.

24. Roayaie S, Blume IN, Thung SN, Guido M, Fiel M, Hiotis S, et al. A system of classifying microvascular invasion to predict outcome after resection in patients with hepatocellular carcinoma. Gastroenterology 2009;137:850-5.

25. Graesslin O, Abdulkarim BS, Coutant C, Huguet F, Gabos Z, Hsu L, et al. Nomogram to predict subsequent brain metastasis in patients with metastatic breast cancer. J Clin Oncol 2010;28:2032-7.

26. Rouzier R, Pusztai L, Delaloge S, Gonzalez-Angulo AM, Andre F, Hess KR, et al. Nomograms to predict pathologic complete response and metastasis-free survival after preoperative chemotherapy for breast cancer. J Clin Oncol 2005;23:8331-9.

27. Landis JR, Koch GG. The measurement of observer agreement for categorical data. Biometrics 1977;33:159-74.

28. McGraw, O. K, Wong SP. Forming inferences about some intraclass correlation coefficients. Psychological Methods 1996;1:30-46.

29. Nishie A, Yoshimitsu K, Asayama Y, Irie H, Tajima T, Hirakawa M, et al. Radiologic detectability of minute portal venous invasion in hepatocellular carcinoma. AJR. American journal of roentgenology 2008;190:81-7.

30. Honda H, Hayashi T, Yoshida K, Takenaka K, Kaneko K, Fukuya T, et al. Hepatocellular carcinoma with sarcomatous change: characteristic findings of two-phased incremental CT. Abdominal imaging 1996;21:37-40.

31. Kierans AS, Leonardou P, Hayashi P, Brubaker LM, Elazzazi M, Shaikh F, et al. MRI findings of rapidly progressive hepatocellular carcinoma. Magnetic resonance imaging 2010;28:790-6.

32. Siripongsakun S, Lee JK, Raman SS, Tong MJ, Sayre J, Lu DS. MRI detection of intratumoral fat in hepatocellular carcinoma: potential biomarker for a more favorable prognosis. AJR. American journal of

roentgenology 2012;199:1018-25.

33. Woodall CE, Scoggins CR, Loehle J, Ravindra KV, McMasters KM, Martin RC. Hepatic imaging characteristics predict overall survival in hepatocellular carcinoma. Annals of Surgical Oncology 2007;14:2824-30.

34. Wu TH, Yu MC, Chen TC, Lee CF, Chan KM, Wu TJ, et al. Encapsulation is a significant prognostic factor for better outcome in large hepatocellular carcinoma. Journal of surgical oncology 2012;105:85-90.

35. An C, Park MS, Jeon HM, Kim YE, Chung WS, Chung YE, et al. Prediction of the histopathological grade of hepatocellular carcinoma using qualitative diffusion-weighted, dynamic, and hepatobiliary phase MRI. Eur Radiol 2012;22:1701-8.

36. Heo SH, Jeong YY, Shin SS, Kim JW, Lim HS, Lee JH, et al. Apparent diffusion coefficient value of diffusion-weighted imaging for hepatocellular carcinoma: correlation with the histologic differentiation and the expression of vascular endothelial growth factor. Korean Journal of Radiology 2010;11:295-303.

37. Nasu K, Kuroki Y, Tsukamoto T, Nakajima H, Mori K, Minami M. Diffusion-weighted imaging of surgically resected hepatocellular carcinoma: imaging characteristics and relationship among signal intensity, apparent diffusion coefficient, and histopathologic grade. AJR, American journal of roentgenology 2009;193:438-44.

38. Nishie A, Tajima T, Asayama Y, Ishigami K, Kakihara D, Nakayama T, et al. Diagnostic performance of apparent diffusion coefficient for predicting histological grade of hepatocellular carcinoma. Eur J Radiol 2010.

<ABSTRACT (IN KOREAN)>

# 자기공명영상을 이용한 단일 간세포암의 근치적 절제술 후 조기재발 위험의 예측

<지도교수 김명진>

연세대학교 대학원 의학과

안찬식

목적: 간절제술은 간세포암의 주된 치료법 중 하나이지만, 수술 후 재발률이 높은 것이 큰 단점이다. 특히 수술 후 2년 내 재발하는 조기재발의 경우 그 이후 재발하는 경우에 비해 예후가 나쁜 것으로 알려져 있다. 따라서 이 연구에서는 자기공명영상 소견들을 종합하여 간세포암의 근치적 절제술 후 조기재발의 위험을 수술 전에 예측하는 모델을 수립하고 이의 유용성을 확인하고자 하였다.

재료 및 방법: 2008년 1월부터 2011년 8월까지 세브란스병원에서 단일 간세포암으로 자기공명영상을 시행하고 근치적 수술을 받은 268명의 환자를 대상으로 연구가 이루어졌다. 2010년 9월 이전에 수술을 받은 187명은 모델수립군으로, 나머지 81명의 환자들은 모델확인군으로 하였다. 모델수립군의 187명 환자의 모든 자기공명영상을 두 명의 영상의학과 전문의가 후향적으로 분석하여 다음과 같은 8가지 항목의 유무를 상호 동의 하에 판단하였다: 동맥기에서 환형 조영증가,

동맥기에서 종양주변 조영증강, 피막, 간췌조영시기에서의 종양주변 간실질의 저신호, 간췌조영시기에서의 종양경계의 불규칙성, 위성결절, 그리고 혈관침범. 종양표지자 등, 수술 전에 확보할 수 있는 임상지표들도 조사하였다. 이러한 변수들을 이용하여 다변량 로지스틱 분석을 시행하였고, 이 결과에 따라 예측모델을 수립하였다. 이 예측모델에 유의한 인자로서 포함된 자기공명영상 소견들만 다시 모델확인군에 속하는 환자들을 대상으로 같은 영상의학과 전문의가 분석을 하여, 수립된 예측모델이 별도의 모델확인군에서도 조기재발을 잘 예측할 수 있는지 확인하였다.

결과: 로지스틱 회귀분석 결과 187명의 모델수립 환자군에서 간세포암의 조기재발과 독립적으로 유의한 관계를 보인 요소는 다음과 같았다: 동맥기에서 환형 조영증가 (odds ratio [OR], 3.83; 95% confidence interval [CI], 1.39-10.52; P=0.01), 동맥기에서 종양주변 조영증강 (OR, 2.64; 95% CI, 1.27-5.46; P<0.009), 위성결절 (OR, 4.07; 95% CI, 1.09-15.21; P=0.037), 그리고 종양의 크기 (OR, 1.66; 95% CI, 1.31-2.09; P<0.001). 이러한 결과를 바탕으로 수립한 예측모델을 이용하여 간절제술 후 간암의 조기재발을 예측하는 데 있어서의 진단능력을 모델수립군에 속하는 환자들을 대상으로 평가하였다. 그 결과 곡선하면적 (area under the curve [AUC])이 0.788이었다. 이 예측모델을 모델확인군에 속하는 81명의 환자들에 적용하였을 때, 0.783의 곡선하면적을 보였으며 이 값은 모델수립군에서의 0.788과 통계학적으로 유의한 차이가 없는 것으로, 모델수립군에서 도출해 낸 예측모델이 모델확인군에서도 잘 적용됨을 확인하였다.

결론: 이번 연구를 통하여 단일 간세포암의 근치적 절제술 후 2년 내 조기재발할 위험을 자기공명영상 소견을 이용하여 수술 전에 예측하는 모형을 수립하고, 별도의 환자군에서도 이 예측모형이 잘 적용되는 것을 확인하였다.

---

핵심되는 말 : 간세포암, 조기재발, 근치적 절제술, 자기공명영상